Available online at www.ijpe-online.com

**International Journal of Performability Engineering**

vol. 15, no. 8, August 2019, pp. 2107-2115
DOI: 10.23940/ijpe.19.08.p10.21072115

# Carrier Frequency Estimation based on Frequency Domain and Wavelet Ridge

Xiang Chen[a], Wei Zhi[b,*], and Yihan Xiao[b]

[a]*State Key Laboratory of Complex Electromagnetic Environment Effects on Electronics and Information System (CEMEE), Luoyang, 471003, China*
[b]*College of Information and Communication Engineering, Harbin Engineering University, Harbin, 150001, China*

**Abstract**

To estimate the carrier frequency of digital signals such as MASK, MPSK, and MQAM under the condition of white Gaussian noise, this paper uses the methods based on frequency domain and wavelet ridge, and two corresponding improved methods are proposed. For the method based on frequency domain, aiming at the problem of poor spectral accuracy and applicability, we propose a method using power spectrum instead of spectrum. Compared with the original method, the simulation consequences express that the improved method reduces the signal-to-noise ratio (SNR) threshold by 5dB. For the method based on wavelet ridge, we propose an improved method to identify the problems of initial iteration parameters, accuracy of results, and divergence points. The simulation consequences illustrate that the improved method reduces the signal-to-noise ratio threshold by 2dB compared with the original method.

*Keywords*: carrier frequency estimation; digital signal; frequency domain; power spectrum; wavelet ridge

(Submitted on March 13, 2019; Revised on April 14, 2019; Accepted on June 16, 2019)



## 1. Introduction

Due to the differences in signal characteristics, modulation technology, and multiplexing technology, the types of signals in space have become more and more complex, and the receiver receives the signals in a cooperative or non-cooperative manner. For non-cooperative communications, there are many examples, such as electronic countermeasures, military information monitoring, and national radio management. In the above scenes, a very important step is to estimate the carrier frequency of the received signal. Accurate carrier frequency estimation is of great help to blind demodulation and signal recognition.

Carrier frequency estimation has been studied by many scholars. In 1974, the maximum likelihood estimation algorithm was developed by Rife et al [1]. In 2005, Morelli et al. used the joint maximum likelihood (ML) estimation method to estimate carrier frequency [2]. In the same year, Ko et al. studied an algorithm that used the maximum likelihood (ML) method to estimate the frequency of frequency hopping signals. [3]. In 2013, Guoyi et al. estimated the parameters through STFT-Hough transform, including carrier frequency [4]. In 2016, characteristics of the cyclic correntropy spectrum were studied by Luan et al. They found the relevance of peaks in cyclic frequencies to the carrier frequency [5]. Chayot put forward a carrier frequency estimation plan that was suitable over multipath channels in 2017, but it was only applicable to CPM signals [6]. Using a time–frequency diagram, Fu et al. studied a method used to estimate arguments of signals [7]. In the frequency domain, by estimating the difference between the specimen position of DFT and the real frequency, Xu et al. studied a frequency estimation algorithm in 2017 [8]. Li et al. proposed another frequency estimator based on DFT fundamentals. When it worked together with other estimators, the computational complexity was reduced, but the performance was not reduced [9]. With the help of wavelet transform and fractional auto-correlation, Jun et al. studied a method to estimate the signal arguments [10].

In this paper, the improved frequency domain method based on the Welch power spectrum and the improved method based on wavelet ridge are used to estimate the carrier frequency of various digital modulation signals. The improved

* Corresponding author.
*E-mail address*: 879978106@hrbeu.edu.cn

algorithm has a lower estimation error.

## 2. Method based on Frequency Domain and Wavelet Ridge

### *2.1. Carrier Frequency Estimation based on Frequency Domain*

Any real signal can be expressed in the following form [11]:

$$x(t) = A(t)\cos(\varphi(t)) \tag{1}$$

If $A(t) \geq 0$, it is called the instantaneous amplitude, and if $\varphi(t) \in [0, 2\pi]$, it is called the instantaneous phase.

The main feature of carrier frequency estimation by the frequency centralization method is to use the spectrum characteristics of signals. This algorithm estimates carrier frequency by calculating the center of the spectrum.

If the sampled signal sequence is $x(n)$, the number of sampling points is $N$ and its discrete Fourier transform is $X(k)$. Then,

$$X(k) = DFT\{x(n)\} = \sum_{n=0}^{N-1} x(n)\exp(-j\frac{2\pi nk}{N}) \tag{2}$$

If $f_s$ is the sampling frequency, the estimated carrier frequency $\hat{f}_c$ can be obtained from the following formula:

$$\hat{f}_c = \left( \sum_{i=0}^{\frac{N}{2}-1} i\left|\mathrm{X}(i)\right|^2 \Big/ \sum_{i=0}^{\frac{N}{2}-1} \left|\mathrm{X}(i)\right|^2 \right) \times \frac{f_s}{N} \tag{3}$$

This method only works well for signals with high spectral symmetry, but not for signals with poor spectral symmetry.

We take 2PSK as an example to introduce the process of carrier frequency estimation by the frequency domain centralization method and its advantages and disadvantages. The spectrum of the 2PSK signal is calculated under 30dB and 0dB signal-to-noise ratios. The parameters are: symbol rate 2000Sps, carrier frequency 8KHz, sampling rate 40KHz, and signal length 2000 points.

As shown in Figure 1, the amplitudes on both sides of the signal spectrum increase significantly at 0dB compared with that at 30dB, that is to say, the estimation effect of this method is greatly reduced at a low SNR. This problem is mainly due to the large tail on both sides of the spectrum at a low SNR. To solve this problem, a power spectrum can be used instead of a spectrum to make the amplitude smoother. Next, we take 2PSK and 2FSK signals as examples to calculate the four power spectra of these two signals. The algorithms used include the periodogram method, Welch method, Yule-Walker method, and Burg method. As shown in Figures 2 and 3, the experimental conditions are consistent with those of the previous group, SNR = 5dB.

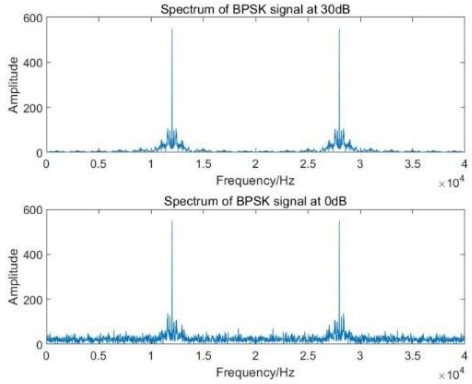


Figure 1. Spectrum comparison of BPSK signal at 30dB and 0dB

From Figures 2 and 3, we can see that the power spectrum can be smoothed well except for the periodogram method. However, through Figure 3, we can see that the four power spectrums of the 2FSK signal have obvious differences. For the effect of smoothing, although the other three methods are better than the method using periodogram, only using the periodogram and Welch method can retain the spectral characteristics of the power spectrum. Therefore, the method based on the Welch power spectrum is employed to improve the performance of anti-noise. Firstly, the power spectrum is calculated by the Welch power spectrum method, and then we estimate the carrier frequency by the frequency domain centralization method.

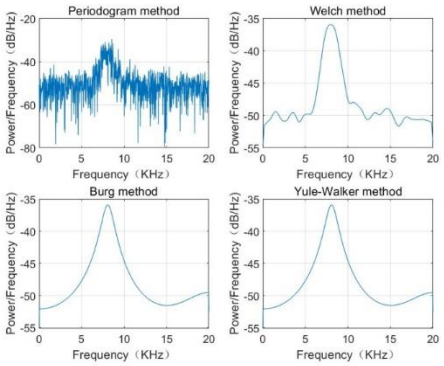


Figure 2. Comparison of several power spectrum of 2PSK signals

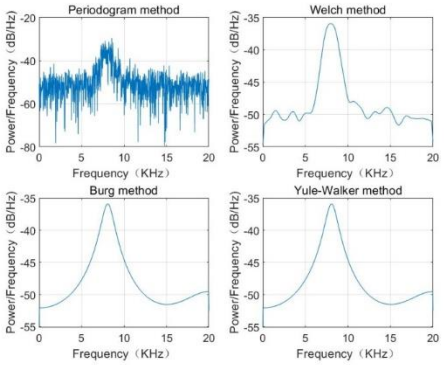


Figure 3. Comparison of several power spectrum of 2FSK signals

### *2.2. Carrier Frequency Estimation based on Wavelet Ridge*

For the signal described in the previous chapter, if $\left|\mathrm{d}\varphi/\mathrm{d}t\right| \gg \left|1/A\right|\left|\mathrm{d}A/\mathrm{d}t\right|$, then $x(t)$ is called asymptotic. The corresponding analytical signal is

$$s(t) = A_x(t)\exp(i\varphi_x(t)) \tag{4}$$

Continuous wavelet transform (CWT) refers to the expansion of functions on the basis of wavelet transform [12]. $b$ is defined as a displacement factor, $a$ is a scale factor, and then its coefficient $WT_s(b,a)$ can be obtained by

$$WT_s(b,a) = \frac{1}{\sqrt{a}}\int_{-\infty}^{+\infty} s(t)g^*\left(\frac{t-b}{a}\right)\mathrm{d}t = \left\langle s(t), g_{(b,a)}(t)\right\rangle \tag{5}$$

The wavelet basis function is $g(t) \in L^2(R)$, and $L^2(R)$ is arbitrary space. If its Fourier transform is $G(\omega)$, then $g(t)$ must satisfy

$$W_\psi = \int_{-\infty}^{+\infty}\frac{|G(w)|}{|w|}\mathrm{d}w < \infty \tag{6}$$

The family of wavelet functions $g_{(b,a)}(t)$ can be obtained by translating and reducing the wave basis function $g(t)$.

$$g_{(b,a)}(t)=a^{-\frac{1}{2}}g\left(\frac{t-b}{a}\right),\ b\in R,\ a>0 \tag{7}$$

Then, the concept of wavelet ridge line should be introduced. It is defined as the point $(a,b)$ on phase plane $\varphi_{a,b}(t)$ that makes the phase stationary point $t_s(a,b)$ zero. From the stationary point $\varphi'_{a,b}(t_s)=0$, the wavelet ridge line $a_r(b)$ can be obtained from

$$a=a_r(b)=\varphi'_{\psi}(0)/\varphi'_s(b) \tag{8}$$

Where $b$ is the translation parameter, $\varphi'_s(b)$ is the derivative of instantaneous phase $\varphi_s(t)$ at point $b$, and $\varphi'_{\psi}(0)$ is the value of the instantaneous phase at zero point after wavelet transform. From this, we can see that the ridge of wavelet can be expressed as $R=\{(a,b)\,|\,a=a_r(b)\}$, which is the function of $b$. The physical concept of the wavelet ridge is expressed as follows: in order to align the transient frequency of the signal at time $b$ with the center frequency of the wavelet transform at the optimal scale, the advantages of multi-resolution and compact support set of the continuous wavelet transform should be brought into play when selecting the optimal scale $a_r(b)$ corresponding to the signal. Thus, the continuous wavelet transform of the signal at the optimal scale can be matched by the wavelet ridge. The instantaneous frequency $f_s(t)$ can be estimated by the wavelet ridge as

$$f_s(t)=\varphi'_s(b)=\varphi'_{\psi}(0)/a_r(b)=w_0/a_r(b) \tag{9}$$

Where $w_0$ is the central frequency of the wavelet basis function. Wavelet ridge $a_r(b)$ can be extracted from the wavelet curve. The wavelet curve is defined as a curve passing through point $\varphi_{a,b}(t)$ on phase plane $\left(a_r(b_0),b_0\right)$ and satisfying point $t_s(a,b)=b_0$. At the intersection of a given wavelet curve and its ridge, the phase angle $\psi(a,b)$ of $\left(W_{\bar{\psi}}Z\right)(a,b)$ has the following characteristics:

$$\frac{\partial\psi(a,b)}{\partial b}\Big|_{t_s(a,b)=b_0}=\frac{1}{a}\varphi'_{\psi}\left(\frac{t_s-b}{a}\right)+\left[\frac{\partial a}{\partial b}\right]\frac{t_s-b}{a^2}\varphi'\left(\frac{t_s-b}{a}\right) \tag{10}$$

$$\frac{\partial\psi(a,b)}{\partial b}\Big|_{t_s(a,b)=b_0}=\frac{\varphi'_{\psi}(0)}{a} \tag{11}$$

The physical concept of the above formula is that when continuous wavelet transform is on a small wave curve, there will be an instantaneous frequency, which is equal to the central frequency of the multi-scale wavelet, and the corresponding central frequency of the multi-scale wavelet will appear when the two intersect. Therefore, the wavelet ridge can be accurately calculated from the phase of its wavelet transform, and by the center frequency of the ridge basis function, the transient frequency of the signal can be obtained.

$$f'_c=\overline{f}_s=\frac{1}{N}\sum_{k=1}^{N}f_s(k) \tag{12}$$

Next, we take the PSK signal as an example to introduce the process of extracting wavelet ridges and estimating carrier frequency. Set the discrete PSK signal model $s(i)$ after sampling as

$$s(i)=A\exp[j(2\pi f_c iT_s+\varphi(i)+\varphi_0)],\ \varphi(i)\in\left[2\pi/M\,(i-1)\right]_{i=1}^{M} \tag{13}$$

In the above formula, $\varphi(i)$ is the phase modulation function that changes with the phase encoding mode, $\varphi_0$ represents the initial phase, $f_s$ is the sampling frequency, $T_s=1/f_s$, $f_c$ is the carrier frequency of the signal, and $A$ is

the constant.

The carrier frequency estimation method in the frequency domain and its improved method are less effective for low signal-to-noise ratios (SNR). From the physical concept of the wavelet ridge introduced above, we know that the modulus maximum position of the corresponding continuous wavelet transform is the wavelet ridge, which is matched filtering of signals under the optimal scale wavelet transform. Therefore, the performance of carrier frequency estimation by the wavelet ridge method will be greatly improved at a low SNR. However, in order to extract the wavelet ridges, it would be a waste of time to search the whole plane when searching the modulus maxima of the wavelet coefficients through the time-frequency plane. In order to lessen the time required for the algorithm, a repeated method is used to obtain the wavelet ridge line in this paper. The iterative method is shown in Table 1.

Table 1. Iterative Method for Wavelet Ridge

| Algorithms: Carrier Frequency Estimation Based on Wavelet Ridge |
|---|
| Input: Time-shift factor $b=kT$, signal sequence $S_k=S(kT)$, sampling period *T*, wavelet transform of fixed stretching and shrinking wave coefficient $a=a_0$ is $\psi_a(k)$, discrete difference factor $D_b$ at $b=kT$, $w_0=\varphi'_\psi(0)$, $\varepsilon=0.05$, signal length *N*. |
| Output: Carrier Frequency Estimate $f_c'$. |
| 1. for *k* = 1 to N |
| 2. $a'=\left\|w_0/\left(D_b\psi_a(k)\right)\right\|$, *n* = 0; |
| 3. while $(a'-a)/a>\varepsilon$ and *n* < 850 do |
| 4. *n* = *n*+1; |
| 5. end |
| 6. $a_r(k)=a'$, $a=a'$, $k=k+1$; |
| 7. end |
| 8. The instantaneous frequency $f_s(k)$ is estimated by using all *k* points $a_r(k)$. Because the instantaneous frequency estimated at the phase jump also has the phenomenon of jump, this paper completes the carrier frequency estimation by means of all point means of $f_s(k)$ and finally obtains the estimated value $f_c'$. |

After using the iteration method, the computational complexity has been greatly reduced, because the iteration method is easy to converge in the calculation and only needs a small range of iteration operations.

According to the above method, we carry out the experiment of wavelet transform and extract the wavelet ridge of the 2PSK signal under ideal conditions. The parameters are: symbol rate 2000Sps, sampling rate 40KHz, signal length 2000 points, and symbol rate 8KHz. The simulation results are demonstrated in Figure 4.

As shown in Figure 4, the estimated instantaneous frequency at the phase jump of the signal also appear to jump. Its shape is similar to "W" and "W, M". We call this phenomenon the "W" law. Taking 2PSK as an example, if the phase mutation value of the signal is defined as $-\pi$ with $2\pi$ as the module, the analysis shows that the negative and positive polarities of the phase mutation correspond to "W, M" respectively if the signal phase mutation is modeled and defined as "W, M". In the simulation of the signal, the abrupt phase value $-\pi$ corresponds to the "W" phenomenon of equal amplitude. It can be concluded that the abrupt phase change and symbol width will have a certain impact on the carrier frequency estimation results.

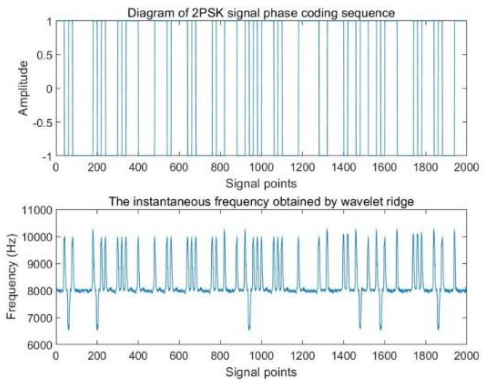


Figure 4. The estimated carrier frequency of 2PSK signal under ideal conditions

According to the above problems, the following improvements are put forward:

1) Firstly, the results of wavelet ridge iteration are improved. When estimating the instantaneous frequency, theoretically, except for the sudden change of the estimated value at the phase mutation, the other instantaneous frequency estimation should be the carrier frequency. However, in the iterative operation of extracting wavelet ridges, noise may have a great impact on the estimation results, so the estimated value can be smoothed first in carrier frequency estimation, thereby reducing the estimation error. Because there are many abrupt changes in the data, if the least square method is used to fit, the results may deviate greatly from the actual values. Therefore, this paper first uses the median filtering method to smooth the estimated value, then obtains the average $f_c'$ after median filtering, and then further smooths the estimated value by setting the corresponding threshold to $f_c'(1\pm\delta)$ and taking $\delta = 0.05$ in the simulation experiment. The final accuracy also has a certain relationship with the size of $\delta$. Finally, all estimations $f_s(k)$ within the threshold are filtered to get the mean. If the number of instantaneous frequency locations after smoothing is $N'$($N'$ < $N$), the formula for calculating the mean value is

$$f_c'' = \bar{f}_s' = \frac{1}{N}\sum_{k=1}^{N'} f_s(k) \tag{14}$$

2) Then, the selection of the initial value $a_0$ of the iteration method is improved. Common methods do not provide any basis and principles for the selection of $a_0$ and usually use empirical values. The large deviation of the initial value will make the estimation result inaccurate due to the non-convergence of the first iteration, and the source is the inappropriate selection of $a_0$. To overcome this conundrum, we propose a method based on frequency domain centralization to estimate the instantaneous frequency of $k$ = 1 time roughly to get $f_s(0)$, and then the initial value $a_0'$ is obtained by

$$a_0' = w_0 / \left(2\pi f_s(0)\right) \tag{15}$$

We keep the experimental parameters unchanged and the experiment at 20dB SNR. The estimated consequences before and after improvement are displayed in Figure 5.

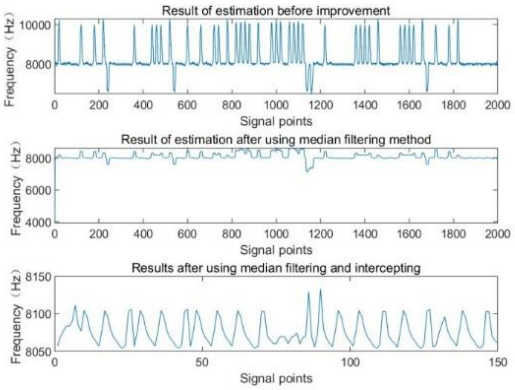


Figure 5. Instantaneous frequency estimation results before and after improvement of 2PSK signal

From Figure 5, it can be seen that the improved instantaneous frequency estimation results have a large span. After mean calculation, the carrier frequency estimation results are 8173Hz. After median filtering, the "W" law at the phase jump can be effectively removed, and after mean calculation, the carrier frequency estimation result is 8100.6Hz. After threshold interception, the span can be further reduced. After mean calculation, the result is 8075.8Hz, which means a more accurate result is obtained. It can be seen that after two steps of improvement, the estimation results have improved to a certain extent.

## 3. Simulation Analysis

Firstly, we take 2PSK as an example to compare the two methods based on frequency domain and wavelet ridge. The experimental results are based on the normalized NMSE to observe the estimation effect. The experimental parameters are:

symbol rate 2000Sps, carrier frequency 4KHz, sampling rate 40KHz, and 100 Monte Carlo experiments at each SNR. The following figure is a comparative experiment of four methods with the signal-to-noise ratio ranging from -15dB to 5dB and keeping the number of symbols unchanged.

As can be seen from Figure 6, the effect of the four carrier frequency estimation methods is obviously improved with the growth of SNR, that is, the value of NMSE gradually decreases. As mentioned above, the improved power spectrum method of the frequency domain centralization method is much better than the original method. When SNR > 0dB, the value of NMSE can fall below 0.001, which is at least 5dB higher than the original method. The wavelet ridge method and its improved method are better than the former two methods, and the improved method is obviously better than the original method. When SNR > -3dB, the value of the NMSE can fall below 0.001, which is 2dB higher than the original method and 3dB higher than the improved method based on the frequency domain method.

Next, four methods under different symbol numbers are compared. The experimental parameters are the same as in the previous experiment. The number of symbols is from 10 to 100. Figure 7 is the estimation curve.

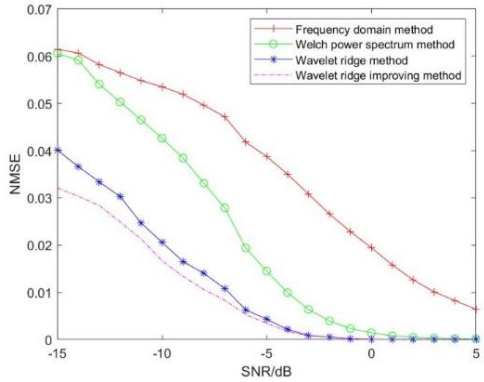


Figure 6. Estimation curves of four carrier frequency estimation methods for 2PSK signals with different SNR

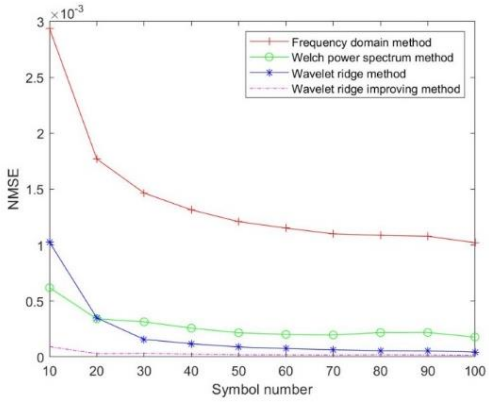


Figure 7. Estimation curves of four carrier frequency estimation methods for 2PSK signals with different symbol numbers

As can be seen from Figure 7, with the increase in the number of symbols, the effect of the four carrier frequency estimation methods gradually improves, that is, the value of the NMSE gradually decreases. However, the change is not very large. The advantages and disadvantages of the four methods are the same as those of the previous experiment. It can be seen that the four estimation methods vary little with the number of symbols in the range of 10 to 100 symbols. That is to say, the influence of the number of symbols on the estimation results of the four methods is less than that of the SNR. This is because when the number of symbols is sufficient to present spectral characteristics, the estimation results will not be affected anymore. The estimation will be influenced only when the number of symbols is small and the spectral characteristics are not obvious enough.

Then, 11 kinds of digital modulation signals are simulated. The experimental parameters are the same as those of the previous experiment. The two improved methods are better than the original method, so only the two improved methods are simulated here. The curves of 11 kinds of signals varying with the SNR are shown in Figures 8 and 9.

As can be seen from Figures 8 and 9, the two carrier frequency estimation methods of 11 signals gradually improve with the growth of SNR, that is, the value of NMSE gradually decreases. Among the two methods, the estimation result of the FSK signal is generally not as good as that of other methods. When the power spectrum method is over 3dB, it tends to gradually stabilize. The value of the NMSE can fall below 0.1. When the wavelet ridge method is above - 5dB, it tends to be stable, and the value of the NMSE can fall below 0.01. Moreover, the estimation effect of the wavelet ridge method is generally better than that of the power spectrum method, because the anti-noise and anti-interference capacity of the power spectrum method is not as good as that of the wavelet ridge method.

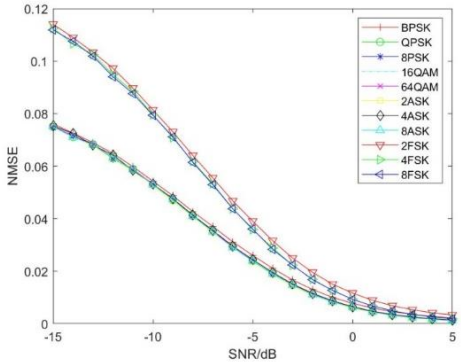


Figure 8. Carrier frequency estimation curves of power spectrum method for 11 signals with different signal-to-noise ratios

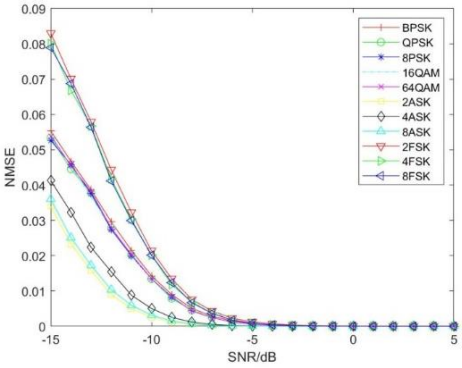


Figure 9. Carrier frequency estimation curve of wavelet ridge improvement method for 11 signals with different signal-to-noise ratios

Finally, the simulation experiments of carrier frequency estimation for 11 kinds of signals with different number of symbols are carried out. The parameters are the same as those of the previous experiments. The number of symbols ranges from 10 to 100. Figures 10 and 11 are the estimation curves of the two improved methods, respectively.

Figures 10 and 11 show that the two estimation methods of 11 signals gradually improve as the number of symbols increases, that is, the value of the NMSE gradually decreases. Among them, when the power spectrum method is used and the number of symbols is above 30, the value of the NMSE can fall below 0.03; when the wavelet ridge method is used and the number of symbols is above 30, the value of the NMSE can fall below 0.002; and when the number of symbols is above 60, the value of the NMSE can fall below 0.001. The wavelet ridge method is generally better than the power spectrum method.

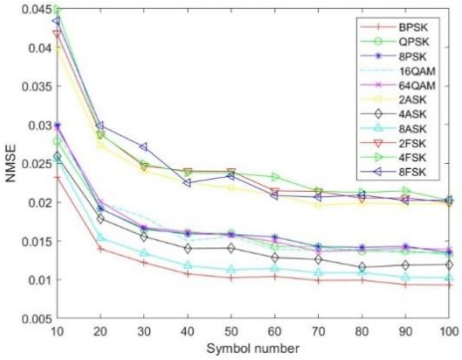


Figure 10. Power spectrum carrier frequency estimation curves for 11 signals with different symbol numbers

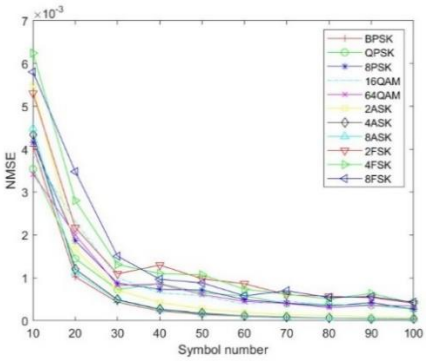


Figure 11. Carrier frequency estimation curve of wavelet ridge improvement method for 11 signals with different symbol numbers

## 4.Conclusions

In this paper, carrier frequency estimation methods based on frequency domain and wavelet ridge are used, and the two methods are improved respectively. The improved method based on frequency domain changes the spectrum of the original method to the Welch power spectrum, and the improved method based on wavelet ridge uses the basic method based on frequency domain as the rough estimation to calculate the initial iteration value and uses the median filter and threshold filter to process the iterated results. The value of the NMSE of the combined method of frequency domain centralization and power spectrum can fall below 0.001 under the SNR > 0dB condition, which is at least 5dB higher than that of the simple method of frequency domain centralization, while the value of the NMSE of the improved wavelet ridge method can fall below 0.001 under the SNR > 3dB condition, which is 2dB higher than that of the original method.

## Acknowledgements

The authors would like to thank the State Key Laboratory of Complex Electromagnetic Environment Effects on Electronics and Information System Director Fund (CEMEE2019K0101A).

## References

1. D. Rife and R. Boorstyn, "Single Tone Parameter Estimation from Discrete-Time Observations," *IEEE Transactions on Information Theory*, Vol. 20, No. 5, pp. 591-598, October 1974
2. M. Morelli and U. Mengali, "Carrier-Frequency Estimation for Transmissions over Selective Channels," *IEEE Transactions on Communications*, Vol. 48, No. 9, pp. 1580-1589, October 2000
3. C. Ko, W. Zhi, and F. Chin, "ML-based Frequency Estimation and Synchronization of Frequency Hopping Signals," *IEEE Transactions on Signal Processing*, Vol. 53, No. 2, pp. 403-410, February 2005
4. G. Y. Zhang, X. L. Qi, X. Z. Zhang, and C. Y. Lin "A Blind Demodulation Algorithm for MFSK Signals using STFT-Radon-Wavelet Transform," in *Proceedings of IEEE International Conference on Green Computing and Communications and IEEE Internet of Things and IEEE Cyber*, *Physical and Social Computing*, pp. 1940-1945, Washington, DC, USA, August 2013
5. S. Luan, T. Qiu, Y. Zhu, and L. Yu, "Cyclic Correntropy and Its Spectrum in Frequency Estimation in the Presence of Impulsive Noise," *Signal Processing*, Vol. 120, pp. 503-508, October 2016
6. R. Chayot, M. L. Boucheret, C. Poulliat, and N. Thomas, "Joint Channel and Carrier Frequency Estimation for Mary CPM over Frequency-Selective Channel using PAM Decomposition," in *Proceedings of International Conference on Acoustics*, pp. 3789-3793, New Orleans, LA, USA, March 2017
7. W. Fu, X. Li, N. Liu, and Y. Hei, "Parameter Blind Estimation of Frequency-Hopping Signal based on Time-Frequency Diagram Modification," *Wireless Personal Communications*, Vol. 97, No. 3, pp. 3979-3992, August 2017
8. C. Xu, L. Zhou, C. Chen, and Q. Zhang, "A Low Computational Complexity Frequency Estimation Method with High Precision of Sinusoid based on DFT," in *Proceedings of International Conference on Information Science and Control Engineering* (*ICISCE*), pp. 1351-1355, Changsha, China, July 2017
9. Y. Li, J. Zhao, J. Li, X. Lei, and Y. Fu, "A New Algorithm for Frequency Estimation based on Frequency Searching," in *Proceedings of International Conference on Digital Signal Processing*, pp. 223-226, Beijing, China, October 2017
10. Z. Qiu, J. Zhu, P. Wang, and B. Tang, "Parameter Estimation of Phase Code and Linear Frequency Modulation Combined Signal based on Fractional Autocorrelation and Haar Wavelet Transform," in *Proceedings of International Conference on Computational Science and Engineering* (*CSE*), *IEEE Computer Society*, pp. 936-939, Chengdu, China, December 2014
11. R. A. Carmona and W. L. Hwang, "Characterization of Signals by the Ridges of their Wavelet Transforms," *IEEE Press*, Vol. 45, No. 10, pp. 2586-2590, November 1997
12. K. Hassan, I. Dayoub, W. Hamouda, and M. Berbineau, "Automatic Modulation Recognition using Wavelet Transform and Neural Network," in *Proceedings of International Conference on Intelligent Transport Systems Telecommunications*, pp. 234-238, Lille, France, October 2010